24th COBEM - 2017

24th ABCM International Congress of Mechanical Engineering
December 3-8, 2017, Curitiba, PR, Brazil

COBEM-2017-0401
EFFECTS OF SOLAR RADIATION IN A DIRECT EXPANSION SOLAR ASSISTED CO_2 HEAT PUMP

Tiago de Freitas Paulino
Graduate Program in Mechanical Engineering, Federal University of Minas Gerais, Av. Antônio Carlos , 6627, Pampulha, 31270-901, Belo Horizonte (MG), Brazil
Department of Materials Engineering, Federal Center of Technological Education of Minas Gerais, Av. Amazonas, 5253, Nova Suiça, 30421-169, Belo Horizonte (MG), Brazil
tfpaulinoeng@gmail.com

Raphael Nunes de Oliveira
Department of Mechanical Engineering, Federal Center of Technological Education of Minas Gerais, Av. Amazonas, 7675, Nova Gameleira, 30510-000, Belo Horizonte (MG), Brazil
rphnunes@gmail.com

Luiz Machado
Ricardo Nicolau Nassar Koury
Graduate Program in Mechanical Engineering, Federal University of Minas Gerais, Av. Antônio Carlos , 6627, Pampulha, 31270-901, Belo Horizonte (MG), Brazil
luizm@demec.ufmg.br, koury@demec.ufmg.br

Abstract. *The superheat in the evaporator outlet, in a direct expansion solar assisted heat pump for water heating, is affected by the modification of solar radiation. In the present work, the mathematical model of the heat pump was used to show the effects of solar radiation in the system. When the model achieves a steady state, the solar radiation was reduced in 5% (simulation 1) and in 15% (simulation 2), consequently the superheat decreased. Ten seconds after the reduction of the solar radiation, the internal area of the expansion device was reduced in 3.5% (simulation 1) and in 9.4% (simulation 2) so that the superheat could return to the initial condition. The reduction of the internal area of the expansion device implies a decrease in the amount of refrigerant mass in the evaporator. Around 50 seconds after the valve step, the superheat had practically returned to the initial condition. It was possible to see that a small modification in solar radiation produces relevant effects on the superheat. Consequently, the expansion device needs to be adjusted almost at the same time for the superheat return to the correct value and the system requires an expansion device with a low response time, as an electronic expansion valve.*

Keywords: *distributed model, solar assisted, direct expansion, superheat, CO_2 heat pump*

1. INTRODUCTION

The direct expansion assisted solar heat pump (DX-SAHP) have widely been used for water heating (Chow *et al.*, 2010; Moreno-Rodríguez *et al.*, 2012 and Omojaro and Breitkopf, 2013). The advantage of this type of equipment is besides receiving energy from natural and forced convection as well as from the condensation of water vapour in the external atmospheric air, the DX-SAHP also receives energy from solar radiation. This larger amount of energy produces an increase in the evaporating temperature and pressure as shows Fig. 1, as a result, the compressor work is lower and the COP of the system rise. Kuang, Sumathy and Wang (2003), Kong *et al.* (2011) and Sun *et al.* (2011) discuss the increase of the COP in a DX-SAHP.

Despite of the possibility of improve the COP, the DX-SAHP is more influenced by the environmental conditions than a non-solar assisted heat pump. During a typical day, the variations of environmental conditions, such as the solar radiation, the ambient temperature and the wind velocity produces changes in the properties of the cycle, including the evaporation temperature and the evaporator outlet superheat. For example, if the system is operating in a steady state and however, the amount of solar radiation is improved, therefore the total amount of energy absorbers in the evaporator / collector is also improved. At this moment, if the same mass flow rate pass through the evaporator / collector the superheat will be increased. In addition, variations of solar radiation occur in both directions, it may

increase in a certain moment and decrease in another. The effects of the superheat variations may be harmful for the system. The increase in superheat may result in the degradation of lubricant oil and as well as in making more difficult for the electric motor to properly cool. On the other hand, the decrease in superheat may result in the liquid being carried over into the compressor. Because of this, in a DX-SAHP, the control of superheat is too important for the proper operation of the system.

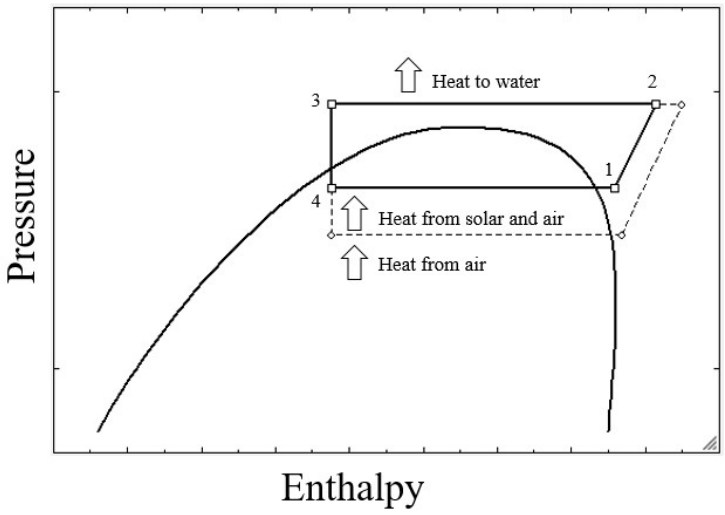

Figure 1: Evaporating temperature and pressure increase in a CO_2 DX-SAHP.

Keeping the superheat at an adequate value can be achieved through the modification of the mass flow rate by the expansion device. The most common expansion devices are the capillary tube, the orifice, the thermostatic expansion valve and the electronic expansion valve. The electronic expansion valve is an adequate device in systems that require a wider working range (Lazzarin and Noro, 2008; Jiang *et al.*, 2011) and a short response time (Maia *et al.*, 2014).

If the heat pump use carbon dioxide (CO_2) as a refrigerant for produce water heating, in general, three variables need to be controlled: the water temperature, the superheat and the optimum high pressure. The optimum high pressure is the most important factor for the system operate at the maximum COP (Kauf, 1999; Qi *et al.*, 2013 and Yang *et al.*, 2015). The simultaneous control of the superheat and the optimum high pressure have been achieved with the use of one back pressure valve for control the optimum high pressure, one thermostatic expansion valve for control the superheat, and between both valves is installed one receiver for ensuring saturation conditions at the thermostatic expansion valve entrance (Peñarrocha *et al.*, 2014). It is important to highlight when the CO_2 heat pump is used to produce hot water for sanitary propose, it operates in a transcritical cycle.

In the present paper, for the propose of study the effect of the solar radiation variation in the superheat, a mathematical model of the evaporator, the expansion device and the compressor for a CO_2 DX-SAHP for water heating is used. Then, to keep the superheat at an adequate value the expansion device have been used for adjust the mass flow rate of CO_2. In order to demonstrate this, two simulations will be performed. In each one a different solar radiation step and valve step are considered. The importance of the control of the water temperature and the COP in a DX-SAHP is not discuss in this paper.

2. MATHEMATICAL MODEL

The main components at this CO_2 DX-SAHP are an evaporator/collector, a reciprocating compressor, a gas cooler and a needle valve as an expansion device. This heat pump is used for water heating and the hot water is storage in a thermal energy storage. The evaporator operation depends of other components in the system, particularly the expansion device and the compressor. The mathematical model of the evaporator/collector, the compressor and the expansion device is presented in this section. The variables have been considered constant in the gas cooler. This model was developed and validated by Faria *et al.* (2016). The subscripts numbers in the follows equations are equivalent as shows Figure 1.

2.1 Expansion device

The refrigerant flow rapidly through the small expansion device because of this the process is consider practically adiabatic and isenthalpic in the steady state. Them the enthalpy is calculated by Eq. (1) and mass flow rate by Eq. (2) as presented Park *et al.* (2007).

$$h_4 = h_3 \tag{1}$$

$$\dot{m}_{ED} = C.A_{orf}\sqrt{2\rho_3\left(P_3 - P_4\right)} \tag{2}$$

Where:

A_{orf}	area of the cross-section needle valve orifice [m²]
C	orifice coefficient
ED	expansion device
h	specific enthalpy [kJ.kg^{-1}]
$\dot{m}$	mass flow rate [kg.s^{-1}]
P	pressure [Pa]
ρ	density [kg.m^{-3}]

2.2 Compressor

The compressor has a small displacement and a high rotational speed, then it operates practically in the steady state. The mass flow rate is calculated by Eq. (3) (Faires, 1983). In this study the volumetric efficiency of compressor is considered equal 70%.

$$\dot{m}_{comp} = N\rho_1 V\eta_v \tag{3}$$

Where:

comp	compressor
N	rotational speed [rps]
V	volumetric displacement [m³.rev^{-1}]
η_v	volumetric efficiency

2.3 Evaporator / collector

The evaporator / collector receives energy from natural and forced convection, from the condensation of water vapour in the external atmospheric air and from solar radiation. Tab. 1 shows the main characteristics and parameters of the evaporator / collector.

Table 1. Characteristics and parameters of the evaporator/ collector.

Geometry	Absorber(fins) and coil (tube)
Tube and fins	Cooper
Secondary fluid	Air
Tube diameters (out/in)	D_o = 7.6 mm and D_i = 6.0 mm
Coil length	L = 16.3 m
Distance between tubes	W = 0.10 m
Fin thickness	δ_{fin} = 1.0 mm
Fin efficiency	η_{fin} = 0.98
Plate area	A = 1.57 m²

In order to model the evaporator it is necessary to consider few simplifying assumptions. These assumptions include considering: (i) in the boiling region the liquid and vapor are in thermodynamic equilibrium; (ii) unidirectional refrigerant flow; (iii) no axial heat conduction; (iv) physical properties of the CO_2 and copper are uniform in each tube cross section; (v) negligible resistance of contact between the coil and absorber and finally; (vi) negligible resistance of the wall tube. Based upon these assumptions the balances of energy, mass and moment for the refrigerant is presented in Eq. (4), (5) and (6), while the balance of energy for the coil is presented in Eq. (7):

$$A_f \frac{\partial}{\partial t}\left[\rho_f\left(h_f - P_f v_f\right)\right] = -A_f \frac{\partial}{\partial z}\left(G_f h_f\right) + H_f p_f\left(T_w - T_f\right) \tag{4}$$

$$\frac{\partial \rho_f}{\partial t} + \frac{\partial G_f}{\partial z} = 0 \tag{5}$$

$$\frac{\partial}{\partial t}\left\{ P_f + G_f^2 \left[\frac{x^2 v_v}{\alpha} + \frac{(1-x)^2 v_l}{1-\alpha} \right] \right\} = -\frac{\partial G_f}{\partial t} - \left(\frac{dP}{dz} \right)_{fr} - g\rho_f \sin(\theta) \tag{6}$$

$$\rho_w A_w c_{pw} \frac{\partial T_w}{\partial t} = \left[(W - D_0) F + D_0 \right] \left[S - U_L \left(T_w - T_{sky} \right) \right] - H_f A_f \left(\mathrm{T_w} - \mathrm{T_f} \right) \tag{7}$$

Where:

A	plate area [m²]
c_p	specific heat at constant pressure [J.kg^{-1}.K^{-1}]
D_0	external diameter [m]
f	refrigerant
F	fin efficiency
g	acceleration of gravity [m.s^{-2}]
G	mass velocity [kg.s^{-1}.m^{-2}]
H_f	heat transfer coefficient between the wall and the refrigerant [W.m^{-2}.K^{-1}]
p	perimeter [m]
S	solar radiation [W.m^{-2}]
T	temperature [K]
sky	sky
T	temperature [K]
U_L	combined coefficient involving radiation and convection between the absorber / coil and the environment [W.m^{-2}.K^{-1}]
v_f	liquid specific volume [m³.kg^{-1}]
v_v	vapor specific volume [m³.kg^{-1}]
x	quality
w	tube wall
W	distance between the centers of two adjacent tubes [m]
(dP/dZ)fr	refrigerant pressure loss by friction [Pa]
α	void fraction
θ	inclination of the absorber relative to the horizontal

The correlations used in equations to calculate heat transfer, void fraction and pressure loss are: (i) *Hf* in the boiling region as proposed by Cheng et al. (2006) and Cheng et al. (2008); and in superheating region with equation of Dittus-Boelter, presented by Incropera and DeWitt (2002); (ii) void fraction as proposed by Rouhani and Axelsson (1970); (iii) pressure loss in the boiling region as proposed by Fridel and recommended by Cheg et al (2008) and in superheating region with equation of Fanning, described by Ozisik (1985); (iv) U_L in the natural convection part is obtained as proposed by Palyvos (2008), and the condensation part is determined as presented by Huhtiniemi and Corradini (1993); and (v) the equations used to obtain the direct and diffuse radiation and the heat exchange by infrared radiation are calculated as proposed by Duffie and Beckman (2006) and Kalogirou (2009). For more details, see Faria et al. (2016).

2.4 Discretization of the evaporator / collector equations

The time-dependent and spatial-dependent derivatives in the refrigerant equations were determined from the Eq. (8) and (9) respectively:

$$\frac{\partial y}{\partial t} = \frac{y - y^0}{\Delta t} \tag{8}$$

$$\frac{\partial y}{\partial z} = \frac{y_o - y_i}{\Delta z} \tag{9}$$

The subscripts *i* and o represent the control volume inlet and outlet respectively. The dependent variable *y* can be temperature, pressure, enthalpy, density, mass flow rate, etc. The variables t and z are the time and the spatial position respectively. And the superscripts *0* represents the values of the variables at the instant of time $t-\Delta t$.

2.5 Simulation methodology

Based on the equations above describe a Fortran program was developed for this distributed model. The CO_2 properties were estimated using the equations proposed by Span and Wagner (1996), the evaporator model was run with 2000 control volumes and a time step of 2 seconds. Figure 2 shows the model flowchart for the procedure follow described.

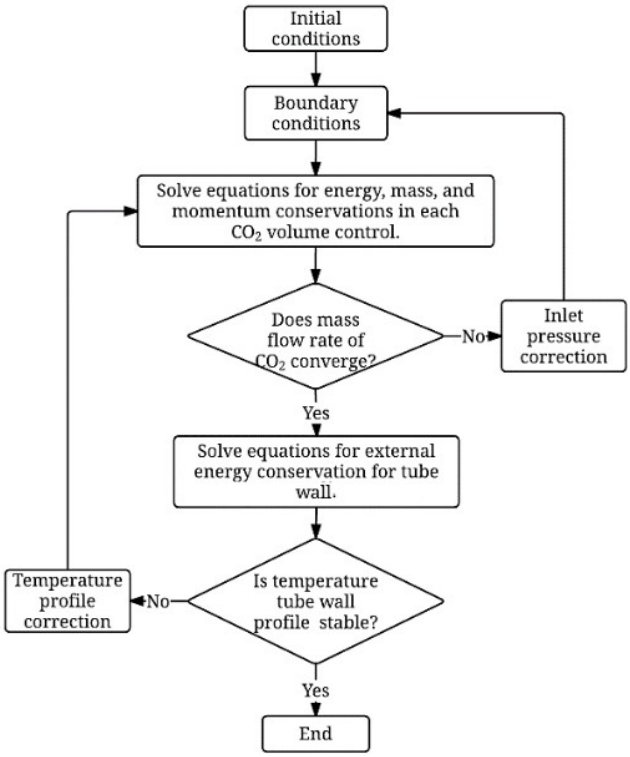

Figure 2. Model flow chart.

First, the boundary and initial conditions are given in the model. The boundary conditions are the environment conditions and the temperature (T3) and pressure (P3) at the gas cooler outlet. Initial conditions are the temperature and enthalpy along the evaporator. Therefore, Eq. (1) calculates the enthalpy (h4) at the evaporator inlet. After that, the spatial profile of the evaporator wall temperature and the expansion device outlet pressure (P4) are assumed, this values are not real and it will use as convergence criterion. Then, Eq. (2) calculates the mass velocity (G4) imposed by the expansion device. For the first evaporator control volume the input data are h4, G4 and P4, then, using Eq. (4), (5) and (6) the output data are calculated. This data are the input for the next control volume, this procedure is used in all evaporator. It is important to highlight the use of different correlations in boiling and superheat region how was discussed in the evaporator model. With the output data of the evaporator last control volume, Eq. (3) calculates the mass velocity (G1) imposed by the compressor. Now, if G4 is not equal to G1, the inlet evaporator pressure need to be changed.

After the second interaction, the Newton-Raphson algorithm is used to accelerate the convergence between the mass velocity given by Eq. (3) and (5), within a defined error margin. The second step of the model is the calculation of the spatial profile of the tube wall temperature by Eq. (7). The procedure for calculating refrigerant properties will be repeated until the convergence of the tube wall temperature. Finally, this procedure is repeated for each instant of time, and during the simulation the boundary conditions could be changed.

3. RESULTS AND DISCUSSION

The DX-SAHP operates at the steady state with 14.4 °C of the evaporating temperature, 6 °C of the superheat, 30 kg/h of the mass flow rate and 670 W/m² of the solar radiation. In order to demonstrate the methodology two simulations were developed and a very similar behaviour were identified for simulations 1 and 2. At 160 seconds, the

solar radiation is reduced (Solar radiation step) in 5% in the simulation 1 and in 15% in the simulation 2. The system response is showed in Fig. 3 and 4 for simulation 1 and in Fig. 5 and 6 for simulation 2. In Fig. 3, as a result of solar radiation reduction the evaporating temperature and pressure is decreased. In addition, in the evaporator / collector the total amount of energy absorbers is reduced and the quantity of mass is the same, then the superheat decrease. Furthermore, in Figure 4 the mass flow rate starts increasing in the expansion device, as describe Eq. (2) for a reduction of outlet pressure in the expansion device. The mass flow rate in the compressor remains almost constant, by Equation 3 is possible to verify it is dependent of the CO_2 density in the compressor inlet, witch value decreases with the reduction of the pressure, but in the other hand increases with the reduction of the temperature. Similarly, Fig. 5 and 6 shows the same behaviour for the simulation 2.

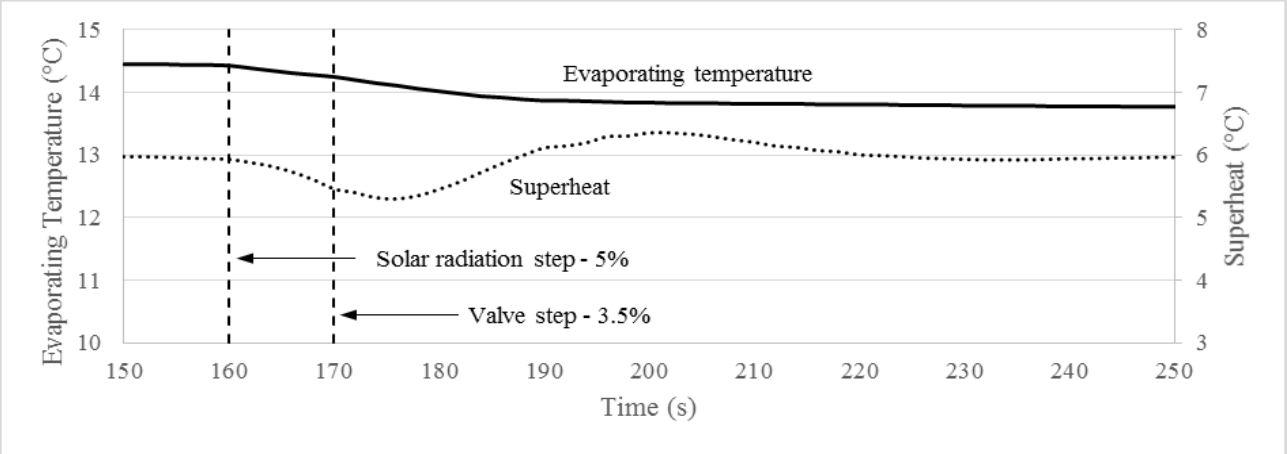

Figure 3. Evaporating Temperature and Superheat Variations – Simulation 1.

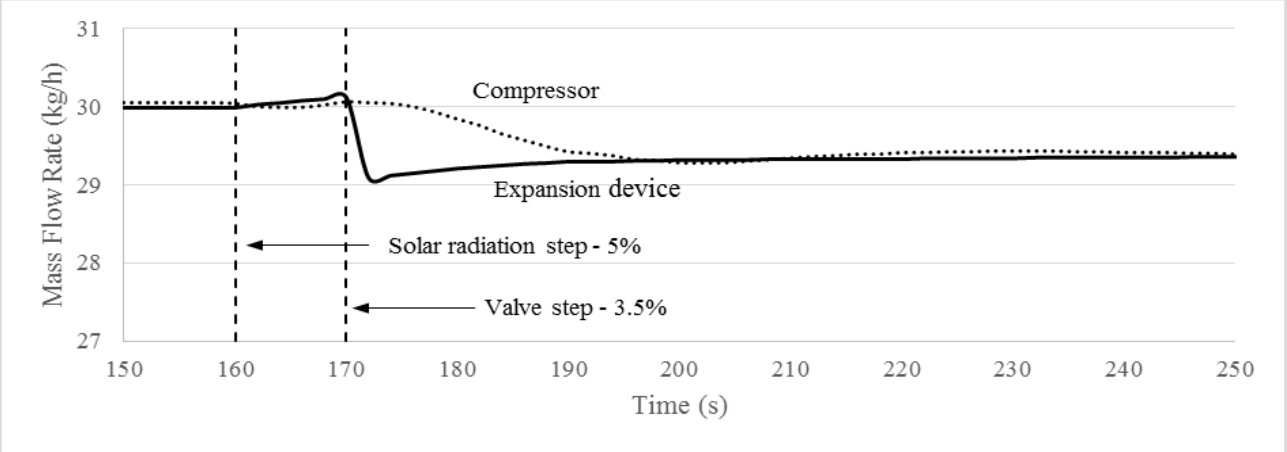

Figure 4. Mass Flow Rate Variations - Expansion Device and Compressor – Simulation 1.

To keep the superheat at an adequate value the expansion device need to be used for adjust the mass flow rate of CO_2. Thus, at the time of 170 seconds, the internal area of the expansion device is reduced (Valve step) in 3.5% in the simulation 1 and in 9.4% in the simulation 2. At that time the mass flow rate through the expansion device reduce very fast as show Fig. 4 and 6. It can be explained by Eq. (2), the reduction of the internal area of the expansion device results in a reduction of the orifice coefficient and consequently the mass flow rate decrease abruptly to a value little lower than 29.1 kg/h (simulation 1) and 27.6 kg/h (simulation 2). Subsequently, the mass flow rate increases until achieve the final value, 29.4 kg/h (simulation 1) and 28.3 kg/h (simulation 2) around 50 seconds after the Valve step. In addition, the mass flow rate imposed by compressor decrease, its happen because the refrigerant density decrease when compressor inlet temperature decrease and it has been occurred slowly.

The difference between the mass flow rate imposed by the compressor and the expansion device cause fluctuation in the superheat as seen Fig. 3 and 5. The superheat achieve the maximum value 6.4 °C (simulation 1) and 7.0 °C (simulation 2) in 200 seconds, but after this value it decreases until stabilizing. If the mass flow rate imposed by compressor is higher the refrigerant inside the evaporator is drying and the superheat increases. On the other hand, if the mass flow rate imposed by expansion device is higher the refrigerant inside the evaporator is flooding and the superheat

decreases. The difference between the two mass flow rates represents the refrigerant being add or remove from the evaporator.

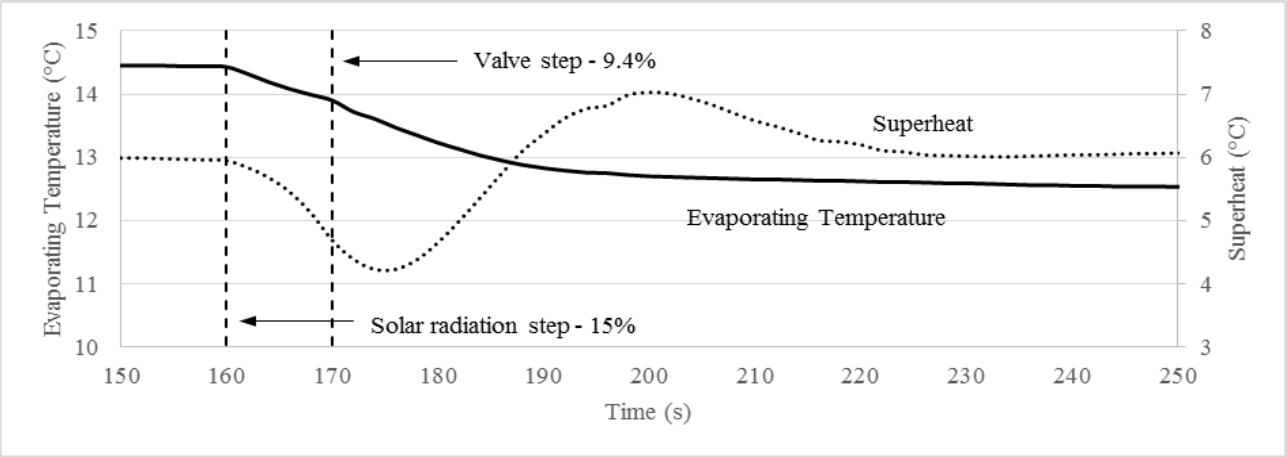

Figure 5. Evaporating Temperature and Superheat Variations – Simulation 2.

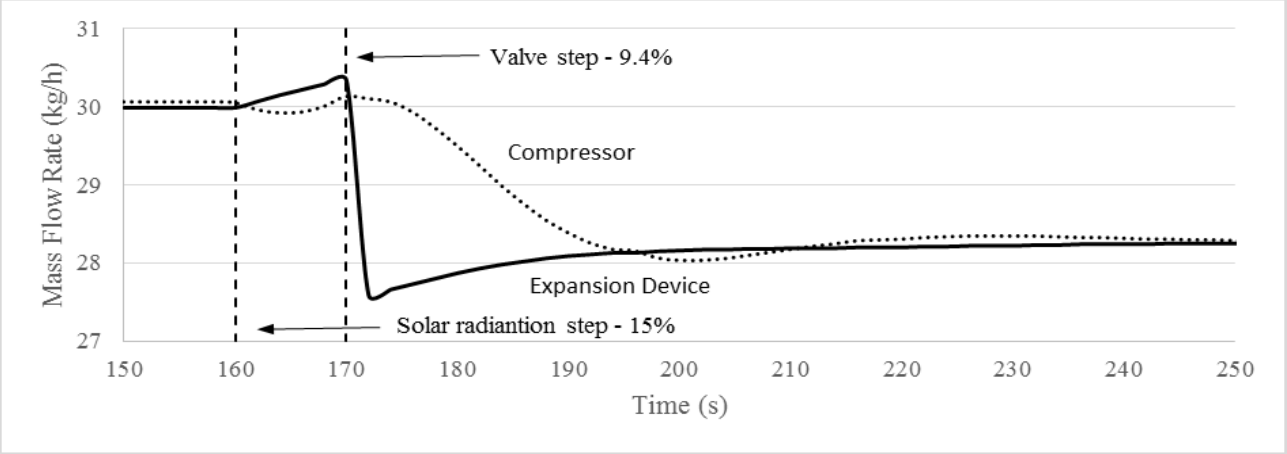

Figure 6. Mass Flow Rate Variations - Expansion Device and Compressor – Simulation 2.

Figure 4 shows that the quantity of mass in the evaporator decrease and after some seconds the superheat starts increasing as demonstrate Fig. 3 and 5. It is necessary around 50 seconds until superheat return to the correct value, 6 °C. As show Fig. 3, the evaporating temperature achieves the final value around 30 seconds after the Solar radiation step, and the Valve step does not affect the evaporating temperature. Further, it is possible to be noted by the slope of the curves that the variation of evaporating temperature is less sharply than the variation of the superheat. Figure 5 and 6 shows similarly behaviour for simulation 2.

In brief, one small variation of the solar radiation affect the superheat almost immediately and could produces dangers results in the DX-SAHP. In order to keep the superheat to its set point, the expansion device needs to be adjusted almost at the same time for reducing the mass flow rate in the system. Then, the direct expansion solar assisted heat pump requires an expansion device with a low response time, as an electronic expansion valve.

4. CONCLUSIONS

This paper presents the use of a dynamic model for DX-SAHP to study the effects of the solar radiation variation. The results show that one small and abruptly variation of the solar radiation affect the superheat almost immediately and could produce dangerous results in a DX-SAHP. In order to keep the superheat to its set point, the expansion device needs to be adjusted almost at the same time for reducing the mass flow rate in the system. Then, the direct expansion solar assisted heat pump requires an expansion device with a low response time, as an electronic expansion valve.

5. ACKNOWLEDGEMENTS

This work was supported by Fundação de Amparo à Pesquisa do Estado de Minas Gerais (FAPEMIG).

6. REFERENCES

Cheng, L., Ribatski, G., Wojtan, L. and Thome, J.R., 2006. "New flow boiling heat transfer model and flow pattern map for carbon dioxide evaporating inside horizontal tubes". International Journal of Heat and Mass Transfer, Vol. 49, p. 4082–4094.

Cheng, L., Ribatski, G., Quibe´n, J.M. and Thome, J.R., 2008. "New prediction methods for CO_2 evaporation inside tubes: Part I – A two-phase flow pattern map and flow pattern based phenomenological model for two-phase flow frictional pressure drops". International Journal of Heat and Mass Transfer, Vol. 51, p. 111–124.

Chow, T.T., Pei, G., Fong, K.F., Lin, Z., Chan, A.L.S. and He, M., 2010. "Modeling and application of direct-expansion solar-assisted heat pump for water heating in subtropical Hong Kong". Applied Energy, Vol. 87, p. 643–649.

Duffie, J.A. and Beckman, W.A., 2006. *Solar Engineering of Thermal Processes*. Wiley, 3rd edition.

Faires, V.M., 1983. Termodinâmica. Tradução de: Thermodynamics. Guanabara Dois, Rio de Janeiro, 6th edition.

Faria, R.N., Nunes, R.O., Koury, R.N.N. and Machado, L., 2016. "Dynamic modeling study for a solar evaporator with expansion valve assembly of a transcritical CO_2 heat pump". International Journal of Refrigeration, Vol. 64, p. 203–213.

Huhtiniemi, I.K., Corradini, M. L., 1993. "Condensation in the presence of noncondensable gases". Nuclear Engineering and Design, Vol. 141, p. 429–446.

Incropera, F.P. and DeWitt, D.P., 2002. *Fundamentals of Heat and Mass Transfer*. John Wiley & Sons, 5th edition.

Jiang, M., Wu, J., Wang, R. and Xu, Y., 2011. "Research on the control laws of the electronic expansion valve for an air source heat pump water heater". Building and Environment, Vol. 46, p. 1954-1961.

Kalogirou, S., 2009. *Solar Energy Engineering: Processes and Systems*. Elsevier, Burlington, 1st edition.

Kauf, F., 1999. "Determination of the optimum high pressure for transcritical CO_2-refrigeration cycles". International Journal of Thermal Sciences, Vol. 38, p. 325-330.

Kong, X.Q., Zhang, D., Li, Y. and Yang, Q.M., 2011. "Thermal performance analysis of a direct-expansion solar-assisted heat pump water heater". Energy, Vol. 36, p. 6830-6838.

Kuang, Y.H., Sumathy, K. and Wang, R.Z., 2003. "Study on a direct-expansion solar-assisted heat pump water heating system". International Journal of Energy Research, Vol. 27, p. 531–548.

Lazzarin, R. and Noro, M., 2008. "Experimental comparison of electronic and thermostatic expansion valves performances in an air conditioning plant". International Journal of Refrigeration, Vol. 31, p. 113-118.

Maia, A.A.T., Horta-Gutierrez, J.C., Koury, R.N.N. and Machado, L., 2014. "Superheating control using an adaptive PID controller". HVAC&R Research, Vol. 20, p. 424–434.

Moreno-Rodríguez, A., González-Gil, A., Izquierdo, M. and Garcia-Hernando, N., 2012. "Theoretical model and experimental validation of a direct-expansion solar assisted heat pump for domestic hot water applications". Energy, Vol. 45, p. 704-715.

Omojaro, P. and Breitkopf, C., 2013. "Direct expansion solar assisted heat pumps: A review of applications and recent research". Renewable and Sustainable Energy Reviews, Vol. 22, p. 33–45.

Ozisik, M.N., 1985. *Heat Transfer, a Basic Approach*. McGraw-Hill, New York.

Palyvos, J.A., 2008. "A survey of wind convection coefficient correlations for building envelope energy systems modeling". Applied Thermal Engineering, Vol. 28, p. 801–808.

Park, C., Cho, H., Lee, Y. and Kim, Y., 2007. "Mass flow characteristics and empirical modeling of R-22 and R410A flowing through electronic expansion valves". International Journal of Heat and Mass Transfer, Vol. 30, p. 1401–1407.

Peñarrocha, I., Llopis, R., Tárrega, L., Sánchez, D. and Cabello, R., 2014. "A new approach to optimize the energy efficiency of CO_2 transcritical refrigeration plants". Applied Thermal Engineering, Vol. 67, p. 137-146.

Qi, P., He, Y., Wang, X. and Meng, X., 2013. "Experimental investigation of the optimal heat rejection pressure for a transcritical CO_2 heat pump water heater". Applied Thermal Engineering, Vol. 56, p. 120-125.

Rouhani, S.Z., Axelsson, E., 1970. "Calculation of void volume fraction in the subcooled and quality boiling regions". International Journal of Heat and Mass Transfer, Vol. 13, n.2, p. 383-393.

Span, R. and Wagner, W., 1996. "A new equation of regime for carbon dioxide covering the fluid region from the triple-point temperature to 1100 K at pressures up to 800 MPa". Journal of Physical and Chemical Reference Data, Vol. 25, p. 1509–1596.

Sun, X., Wu, J., Dai, Y. and Wang, R., 2014. "Experimental study on roll-bond collector/evaporator with optimized channel used in direct expansion solar assisted heat pump water heating system". Applied Thermal Engineering, Vol. 66, p. 571-579.

Yang, L., Li, H., Cai, S., Shao, L. and Zhang, C., 2015. "Minimizing COP loss from optimal high pressure correlation for transcritical CO_2 cycle". Applied Thermal Engineering, Vol. 89, p. 656-662.

7. RESPONSIBILITY NOTICE

The authors are the only responsible for the printed material included in this paper.